Time dependent Monte Carlo simulations of H reactions on the diamond {001}(2×1) surface under chemical vapor deposition conditions

E. J. Dawnkaski,[a] D. Srivastava, and B. J. Garrison
Department of Chemistry, The Pennsylvania State University, University Park, Pennsylvania 16802

(Received 26 January 1995; accepted 13 March 1995)

Time dependent Monte Carlo (TDMC) simulations are performed to determine the effects of a variety of H reactions at a diamond {001}(2×1) surface exposed to gaseous atomic and molecular hydrogen under chemical vapor deposition conditions. The simulation time in the TDMC method is the same as the real time measured in experiments because all of the considered reactions are allowed to occur with probabilities which are the product of the TDMC time step and the corresponding reaction rates. The reaction rates are either explicitly calculated via molecular dynamics or transition state theory methods, or taken from experimental measurements. The simulation takes into account H adsorption, H abstraction, H_2 desorption, H diffusion, and the reverse of these reactions. The relative values of the calculated rates and how they affect the surface radical density and distribution, as well as the effect of CH_3 on radical site diffusion are discussed. © *1995 American Institute of Physics.*

I. INTRODUCTION

Diamond growth via chemical vapor deposition (CVD) is now a well-established process[1–3] and extensive theoretical work has gone into understanding many of the principal phenomena associated with it.[4–13] In spite of these efforts the mechanisms of diamond film growth are not yet fully understood. The CVD growth of diamond films on a hydrogen terminated diamond substrate typically occurs in a gaseous hydrogen/hydrocarbon atmosphere at pressures between 20–30 Torr. The atomic hydrogen in the gas phase is in a dynamic equilibrium with other gas phase species and the diamond surface. The growth process itself is initiated by the formation of a surface carbon radical.[1–13] The most likely means of surface radical formation is the abstraction of a surface H atom by a gas phase H atom to form gaseous H_2. Once the surface radical is formed, gas phase hydrocarbon species such as methyl radical or acetylene can adsorb onto the surface and incorporate into the diamond lattice. The events leading to film growth are hence dependent on the behavior of the surface radical; specifically, how it is created, what events it experiences during its lifetime, and how it is destroyed. The rates of the individual reactions, however, are at best difficult to determine experimentally. One strategy to overcome this problem has been to model the whole growth process with a series of plausible and well-characterized reactions, typically extracted from the gas phase hydrocarbon literature.[5] This assumes that the rates of the gas phase processes are transferable to corresponding surface processes. There exists some evidence that this assumption is not valid at least for the case of H abstraction from the diamond {111} surface.[14] The alternative is to either calculate the individual rates associated with the growth processes or use experimental surface rates if the particular process has been measured. The rates thus determined can then be used in time dependent Monte Carlo (TDMC) procedure in order to extend the microscopic rates of the individual reactions to the macroscopic regime of diamond film growth. The TDMC method which we have been developing[15,16] combines molecular dynamics (MD) simulations for extracting reaction probabilities and mechanisms,[17] simplified transition state theory (TST) for determining reaction rates of activated processes,[18,19] and the TDMC simulations for extrapolating the short-time microscopic information to the macroscopic regime of experimental conditions.[15,16]

The realistic modeling of atomic systems by way of kinetic,[20–24] and time dependent MC simulations[15,16,18,19,25–29] has recently seen two significant developments. First, it is now possible to accurately determine the energetics of the equilibrium configurations as well as the transition barriers of complex systems.[15,16] Thus the rates of individual microscopic processes or reactions can be determined using methods such as molecular dynamics simulations or transition state theory.[18] Second, the definition of the Monte Carlo time and its relationship with real experimental time has been rigorously sought.[15,16,19,25–29] In the case of a single isolated reaction the reciprocal of the reaction rate determines the time required for the reaction to occur.[15,18] This quantity can be set equal to the Monte Carlo time thus defining a direct relationship between the Monte Carlo time and real time. In the case of a many-particle multiprocess system, however, the correlation between the two times is not straightforward. One approach at determining this relationship has been to scale the MC time by a normalization constant chosen such that the MC time matches the experimental time for the simulation of interest.[20–24] Other approaches involve either considering the inverse of the net total reaction rate as a time step and moving one particle at a time,[18,19] or assigning to each particle in the system independent time steps and the real time step is represented as an average over all the independent time steps.[25–27,29] Recently we have presented a simpler alternative,[16] for many-particle multiprocess systems, which is analogous to the single isolated reaction discussed above. Given a set of rates for all the particles and processes in a system, where the reciprocal of a

[a]Department of Chemistry, College of William and Mary, Williamsburg, Virginia 23185.

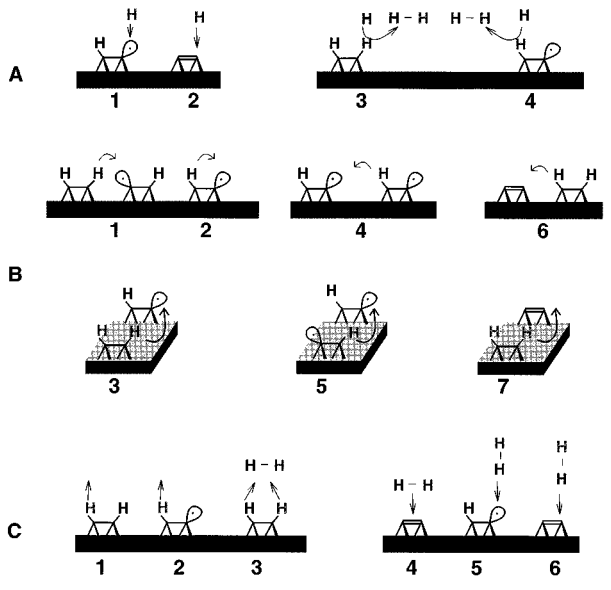

FIG. 1. Schematic diagram of all of the H processes considered in the TDMC calculation. (A)1, H adsorption to an isolated radical; 2, H adsorption at a π-bond; 3, H abstraction to form an isolated radical; 4, H abstraction to form a π-bond; (B), H diffusion process; 1, across trough; 2, across dimer; 3, along dimer row; 4, across trough and form π-bond; 5, along dimer row and form π-bond; 6, across trough and break π-bond; 7, along dimer row and break π-bond; (C)1, H desorption to form isolated radical; 2, H desorption to form π-bond, 3, H_2 desorption; 4, dissociative H_2 addition; 5, H_2 deposition of H at isolated radical; 6, H_2 deposition of H at π-bond.

rate represents the duration of a process, any constant time step may be chosen which is less than the duration of the fastest process. This simulation time step is equivalent to a real time step in which all particles are allowed to move, but the processes are chosen randomly and allowed to occur probablistically as will be explained below.

The processes on the diamond {001}(2×1) surface, shown schematically in Fig. 1, which have been considered in this paper include H adsorption and abstraction reactions, H diffusion, H desorption, H_2 desorption, as well as the reverse of each process so as to satisfy the principle of microscopic reversibility. This represents a large manifold of processes with time scales varying over orders of magnitude. Molecular dynamics simulations using an empirical interaction potential[30] are used to directly determine the probabilities of fast time scale events such as adsorption and abstraction. The rates of slow time scale events such as diffusion and desorption are obtained through the use of transition state theory using the same potential. The rates of both the short and long time scale processes are then combined in the TDMC simulation where two reactive elements, hydrogen and carbon, are present. In addition to the presence of single radical sites on the H-terminated {001}(2×1) surface the simulations result in formation of strained π-bonds[31,32] on individual dimers in equilibrium conditions. The strained π-bonds have been proposed as distinct reaction species on the diamond surfaces[16,33] but their formation and observation in a dynamically equilibrated system has been explored in this work. Our results show that the isolated radical density is from 4%–40% of the total number of C sites and the π-bond density is 1%–10% of the number of surface dimers. This calculation sets the stage for further studies that include hydrocarbon molecular reactions leading to the growth of several layers of diamond under CVD conditions. These results will be published elsewhere.[34]

As the method combines many discrete pieces, this article will be organized with the calculations of the individual reaction rates along with the discussion of the calculated values being described first in Sec. II. The TDMC procedure with the results of the simulations are presented in Sec. III.

II. MICROSCOPIC PROCESSES: RATES AND PROBABILITIES

The dynamic picture of the diamond {001}(2×1):H surface in equilibrium with atomic and molecular hydrogen gas at a given temperature and pressure is composed of microscopic individual reactions as well as the overall macroscopic view of the steady state conditions. The H atoms and the H_2 molecules in the gas phase react with the surface hydrocarbon species and radical sites such that new radical sites are created and previously created ones are destroyed. During the process, radical sites may also diffuse along the surface and come together or scatter off of each other. In this section we describe, in detail, how the rates and probabilities of each of the microscopic reactions are calculated.

Given a realistic interatomic potential function capable of describing the dynamics in a many-particle multiprocess system, ideally one would like to use MD to either study the full dynamics of the system or compute the rates and probabilities of the required microscopic reactions. This is primarily because once the interaction potential has been specified MD does not require any further approximation or knowledge about the paths or the products of the possible reactions under nonequilibrium conditions. For activated reactions with large barriers (~0.5 eV), however, it is challenging to use MD to describe the system because the reaction simply does not occur within the time scales of typical MD simulations (~100 ns). The alternative then is to use transition state theory (TST) for computing the reaction rates, but the reactants and products are predetermined and only the transition states need to be found in the multidimensional phase space. There are cases, however, in which the energetics and structure of the transition states are not easily determined. For these processes we use experimental rates and probabilities or simple estimates. In this section we describe H atom adsorption and abstraction via MD simulations, H atom diffusion via transition state theory, and H and H_2 desorption via experimental observations. The rates of all the reverse processes are obtained from the corresponding forward rates.

A. MD calculations for H atom adsorption and abstraction

We have used molecular dynamics to perform a series of classical trajectory calculations involving H atoms colliding with a diamond {001}(2×1):H surface in order to determine the adsorption probability on a radical site and the abstraction probability from a surface C–H bond [Fig. 1(A)]. The classical trajectory simulation involves solving Hamiltons equations of motion using an analytic potential energy func-

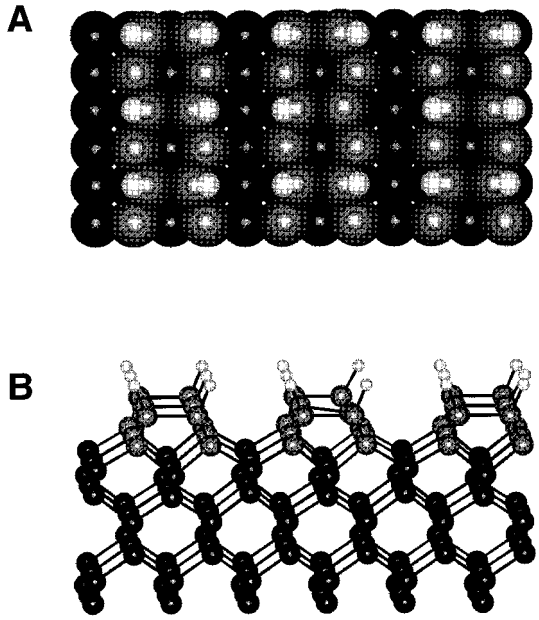

FIG. 2. The diamond {001}(2×1) surface with a surface hydrogen coverage of Θ=0.94. (A) Top view with touching radius spheres. (B) Side view, ball and stick model. If the remaining H atom on the central surface dimer was missing, there would be a strained π-bond.

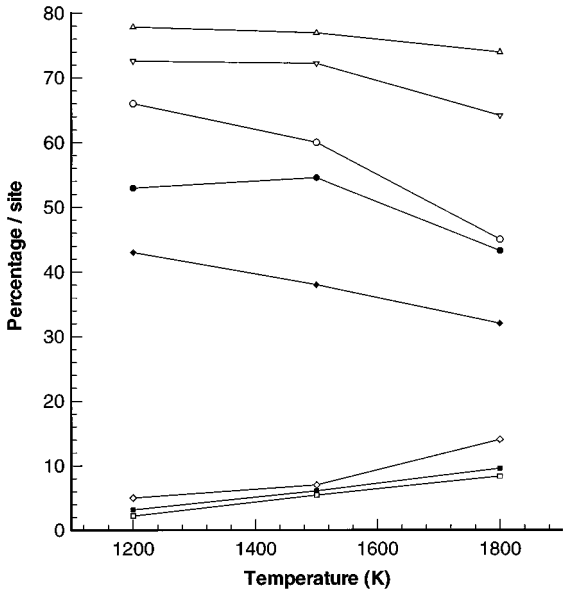

FIG. 3. H adsorption and H abstraction probabilities for the Θ=0.75 {111} surface and several coverages on the {001}(2×1) surface; □, abstraction from {001} Θ=0.89; ■, abstraction from {001} Θ=0.50; ◇, abstraction from {111}; ◆, adsorption {111}; ●, adsorption {001} Θ=0.50; ○, adsorption {001} Θ=0.94; ▽, adsorption {001} Θ=0.89; △, adsorption {001} Θ=0.00.

tion. The specific potential energy function we have used is a many-body empirical bond order potential developed by Brenner.[30,35] This potential was originally developed to model the chemical vapor deposition of diamond films but, in fact, has been used in a number of simulations of other hydrocarbon interactions and reactions including the insertion of CH_2 into a surface dimer on the diamond {001}(2×1):H surface;[17] the pick-up of a molecule from a surface by another gas-phase molecule (and Eley-Rideal reaction sequence);[36] surface molecular reactions during sputtering;[37–41] and compression,[42] indentation,[43,44] and reaction[45–49] at diamond surfaces.

The adsorption and abstraction trajectory studies are performed on a diamond {001}(2×1) crystal with various H atom coverages. The basic system is 8 layers deep with 18 C atoms in each layer. For the (2×1) reconstruction this yields 3 rows of 3 dimers on the surface (see Fig. 2). The bottom two layers of the crystal are held rigid, the next four layers are a heat bath using a Berendsen[50] scheme to maintain the temperature of the system, and the top two layers of C atoms move only under the influence of the interaction potential. Four different surfaces have been prepared that differ only in the hydrogen coverage, Θ. The four configurations are as follows:

(1) Θ=0 (clean π-bonded surface),
(2) Θ=1/2 (each surface dimer has one adsorbed H atom),
(3) Θ=0.89 (a fully hydrogenated surface with one π-bond),
(4) Θ=0.94 (a fully hydrogenated surface with one isolated radical).

Each of these surfaces is equilibrated to the desired temperature for approximately 2 ps. On each surface 6 sets of 400 trajectories for a total of 2400 trajectories are completed. This is done for each of three temperatures, 1200, 1500, and 1800 K. In between each set of 400 trajectories, the surface is further equilibrated for approximately 2 ps. During each individual trajectory a H atom is randomly placed above the crystal and given a thermal velocity picked from a 3D Boltzmann distribution at the same temperature as the substrate. Only the trajectories with net velocities toward the surface are allowed to proceed. The impact zone is thus the entire crystal surface as periodic boundary conditions are employed. The trajectory is then followed until either the H atom reflects from the surface and passes outside the potential cutoff, a hydrogen atom abstraction takes place and the newly formed H_2 molecule passes outside the potential cutoff, or approximately 2 ps has passed. At the end of 2 ps if a reflection or abstraction event has not occurred the incoming atom is checked for adsorption. It is considered adsorbed if it is within 1.8 Å of a surface radical site and if the H binding energy has increased by ~3.4 eV for adsorption onto a π-bond and ~4.0 eV for adsorption onto an isolated radical. Examination of individual trajectories has shown that within 2 ps all impinging H atoms have either adsorbed, reflected, or abstracted.

1. H adsorption

The results from the MD simulations of H atom adsorption on the {001}(2×1) surface of diamond for the four H coverages are given in Fig. 3. Also shown are the values from a similar calculation on diamond {111} in which there were four carbon sites, three of which had H atoms adsorbed and one was a radical site.[51] In all cases the adsorption prob-

TABLE I. Probabilities of H atom and CH_3 dynamics on the diamond {001} (2×1):H surface.

Reaction		Probability (events per μs) 1200 K	1500 K	1800 K
H atom collision (0.1 Torr)	D	$6.56E-02$	$5.87E-02$	$5.36E-02$
H_2 collision (18 Torr)		8.35	7.47	6.82
H atom adsorption				
At an isolated C radical	$A1$	0.0348	0.0320	0.0231
At one C atom in π-bond	$A2$	0.0511	0.0451	0.0396
H atom desorption				
To form an isolated radical	$C1$	$2.49E-12$	$1.31E-08$	$3.96E-05$
To form π-bond	$C2$	$3.94E-08$	$3.00E-05$	$2.50E-03$
H atom abstraction				
To form an isolated radical	$A3$	$1.44E-03$	$3.18E-03$	$4.47E-03$
To form π-bond	$A4$	$2.07E-03$	$3.56E-03$	$5.12E-03$
H_2 deposition of a H atom				
At an isolated radical	$C5$	$2.60E-04$	$1.07E-03$	$2.28E-03$
At one C atom in π-bond	$C6$	$4.68E-08$	$9.06E-07$	$6.54E-06$
H_2 desorption	$C3$	$6.51E-07$	$2.82E-04$	0.0162
H_2 adsorption	$C4$	$1.90E-12$	$8.43E-09$	$2.22E-06$
H atom hop to a radical site				
Across dimer	$B2$	0.0709	3.81	54.3
Across trough	$B1$	$2.89E-05$	$7.61E-03$	0.312
Parallel to trough	$B3$	$4.84E-04$	0.0609	1.53
H atom hop to form a π-bond				
Across trough	$B4$	$7.91E-05$	0.0174	0.637
Parallel to trough	$B5$	$1.62E-04$	0.0256	0.752
H atom hop to break a π-bond				
Across trough	$B6$	$4.19E-09$	$6.52E-06$	$8.75E-04$
Parallel to trough	$B7$	$1.04E-08$	$1.12E-05$	$1.18E-03$
CH_3 hop to a radical site				
Across dimer	$B2$[a]	44.7	368	1499
Across trough	$B1$[a]	$4.86E-03$	0.192	2.22
Parallel to trough	$B3$[a]	0.512	8.31	53.2

[a]Diffusion hops for a CH_3 radical.

abilities are given on a per site (i.e., single C atom with a radical) basis. The following analysis can be made from these values:

(a) The adsorption process is exothermic and unactivated, therefore the absolute value of the adsorption (or sticking) probability represents a measure of the surface area occupied by a surface C radical. The adsorption probability on the {001}(2×1) surface, where each unit cell is 6.37 Å^2, ranges from 50%–75%, thus the adsorption cross section is 3.2–4.8 Å^2. On the {111} surface the unit cell is 5.53 Å^2, the adsorption probability is approximately 40%, thus the cross section is ~2.3 Å^2. The difference is presumably because the radical on the {111} face is perpendicular to the surface whereas on the {001}(2×1) face the radical is at an angle and there is a greater angle of approach for the incoming H atom which can lead to adsorption.

(b) The temperature dependence of the adsorption probability is minor although the greater vibrational motion of the solid at higher temperatures does decrease the probability slightly.

(c) The adsorption onto a π-bond has a greater probability than the adsorption onto an isolated radical. This trend is reverse of the exothermicities as energy must be expended to break the π-bond. The major factor leading to a difference in π-bond adsorption vs isolated radical adsorption is that the portion of the surface available for sticking to the π-bond is greater. Moreover, the empirical potential does not include explicit electron density. The π-bond electron density should, in fact, extend farther above the surface than the electron density of the isolated radical. This would lead to the π-bond sites having even greater reactivity than the isolated radicals towards incoming particles.

(d) There is cooperativity for adsorption among adjacent single radicals or π-bond sites. This is evidenced by the adsorption probability being greater for the clean surface than for the single π-bond. This effect has been observed before for F adsorption on Si (Ref. 52) where, as mentioned above, there is a greater area on the surface where the atom can approach a binding site unhindered.

In the TDMC calculations we have used the adsorption probabilities for the $\Theta=0.5$ case for adsorption onto an isolated radical and those for $\Theta=0$ for adsorption onto the π-bond sites.

2. H abstraction

The H abstraction probabilities are also given in Fig. 3 for both the {100}(2×1) and {111} surfaces. The values shown at each temperature are identical within statistical

limits although the values might be slightly higher for the {111} surface.[51] The activation energy for abstraction is in the range of 0.34–0.42 eV depending on the surface and the coverage. The transition state on both surfaces is a nearly collinear configuration, and is the main reason for the low abstraction probabilities.[51,53] As the temperature of both the gas and surface increases, it becomes easier to overcome the activation barrier and the abstraction probability increases.

3. H collision frequency

The quantities calculated from the MD simulations for H atom adsorption and H atom abstraction to form H_2 are the on-site reaction probabilities that are equivalent to isolated rate constants. What is ultimately needed are the rates for these events which depend on the partial pressure of the ambient gas. The multiplicative conversion factor to do this is the number of collisions per unit time, Z, that the gas particles make with the surface. The collision number is given by[54]

$$Z = A_s P / \sqrt{(2\pi m k_B T)}, \tag{1}$$

where A_s is the area of the site, P is the partial pressure of the gas, m is the mass of the particle, k_B is Boltzmann's constant, and T is the temperature. In this case m is the mass of the H atom and P is the partial pressure of the H atoms above the substrate. A typical value for the H atom partial pressure is 0.1 Torr.[55] A range of values for the H atom partial pressures are used in the final TDMC simulations and the probabilities for H atom adsorption and abstraction under these conditions are listed in Table I.

B. Transition state theory for diffusion

The diffusion of species on the surface occurs concurrently with the adsorption and abstraction events. Using the Brenner hydrocarbon potential and a steepest descent path (SDP) algorithm[56] we have calculated reaction paths for several H atom diffusion processes on the diamond{001}(2×1):H surface [Fig. 1(B)]. We have considered three simple H atom diffusion hops that may occur on this surface; (1) a hop to a radical site on the same dimer; (2) a hop to a radical site on an adjacent dimer across the trough; and (3) a hop to a radical site on an adjacent dimer in the same dimer row. Processes (2) and (3) have also been considered for cases where they cause a π-bond on the surface to be formed or broken [Fig. 1(b)4–7]. Although the primary focus of this study is H concentration and distribution on the surface, the effect of competing reaction processes is also of interest. Therefore the same types of hops for a single isolated radical have also been considered for the case of CH_3 diffusion. Activation barriers for each diffusion path are determined directly from a SDP calculation. The corresponding rate constants are calculated using a simplified transition state theory,[15,18] in which the temperature dependent rate constant is given by

$$k_{\mathrm{TST}} = \nu \exp(-E_a / k_B T). \tag{2}$$

The prefactor, ν, and the activation energy, E_a, are calculated from the same interaction potential as is used for the MD simulations. A description of the methodology used here is given in recent references and will not be delineated here.[15,18] Finally, we assume that the individual hops are isolated events, thus the rate is independent of concentration and the rate equals the rate constant for the specific hop under consideration.

TABLE II. H and CH_3 diffusion activation energies and prefactors.

Reaction		H atom ν (s^{-1})	H atom E (eV)	CH_3 ν (s^{-1})	CH_3 E (eV)
Hop to a radical site					
Across dimer	$B2$	$3.18E+13$	2.06	$1.69E+12$	1.09
Across trough	$B1$	$3.62E+13$	2.88	$4.64E+11$	1.90
Parallel to trough	$B3$	$1.53E+13$	2.50	$5.73E+11$	1.44
Hop to form a π-bond					
Across trough	$B4$	$4.13E+13$	2.79		
Parallel to trough	$B5$	$1.63E+13$	2.62		
Hop to break a π-bond					
Across trough	$B6$	$3.82E+13$	3.80		
Parallel to trough	$B7$	$1.51E+13$	3.61		

Presented in Table II are the activation energies (E_a) and prefactors (ν) for the various diffusion events as calculated from TST. In this calculation the CH_3 is only allowed to migrate within a united molecule approximation, i.e., no H transfer is allowed to occur between the migrating methyl group and the remaining system. Moreover, the CH_3 values are only used with single radical simulations, thus no π-bond states are allowed. Studies underway, though, do include these additional configurations.

Focusing first on the H atom hops we find that all of the activation barriers are quite high at 2–4 eV in contrast to the diffusion of H on metal surfaces. The easiest motion is the migration across the surface dimer (1,2 radical shift), a reaction unprecedented in small molecule chemistry.[57] For the {001}(2×1):H surface it leads to no real net motion, but it is included for completeness.[58] The most difficult motions are to break a π-bond as the π-bond is more stable by 1 eV than two isolated and noninteracting radicals using this interaction potential. The prefactors for H diffusion are nearly constant at a value of 10^{13} hops per s.

Due to the directionality of the C–H bonds it has been argued[59] that diffusion across the trough should be considerably more facile than diffusion parallel to the trough in contrast to the energies calculated with this interaction potential. All the activation energies for H diffusion correspond to almost breaking a surface C–H bond. This is a consequence of the short ranged nature of the interaction potential.[35] Alternatively, dihydride species (i.e., single C atoms with 2 bonded H atoms) could provide a low energy path for diffusion across the trough. In the TDMC calculations some variation of the calculated diffusion barriers is performed to explore the changes in the final results due to the above reasons.

Finally the activation energies and prefactors for CH_3 diffusion are found to be smaller than for H diffusion. The CH_3 molecule is physically larger and should have an extended electron density. Hence it is easier for the CH_3 to

TABLE III. Exponential factors for determining reverse reaction rate constants.

Forward reaction		ΔE (eV)	1200 K	1500 K	1800 K
H_2 desorption to form π-bond	$C3$	−3.14	6.5E−14	2.8E−11	1.6E−09
H abstraction from H saturated dimer	$A3$	−0.33	4.1E−02	7.8E−02	1.2E−01
H abstraction from isolated radical	$A4$	−1.66	1.1E−07	2.6E−06	2.2E−05

bridge the diffusion path length both across and parallel to the surface dimer.

C. Molecular and atomic H desorption

The desorption of H atoms and H_2 molecules from a diamond surface have large activation barriers, thus the rates are too slow to be directly modeled via MD simulations and the short range nature of the interaction potential precludes determining a reasonable transition state for the H_2 desorption reaction. For H atom desorption, an event which has not been observed experimentally, a simple Arrhenius form is assumed where the activation energy is the bond strength as determined from the interaction potential and the prefactor is assumed to be 10^{13} events per s. The rate constant of H atom desorption from a surface dimer with two H atoms bonded is $k=10^{13}\exp(-4.42\ \text{eV}/k_BT)\ \text{s}^{-1}$, where the product is an isolated radical. The H atom desorption from a surface dimer that already has a radical, a rate constant of $k=10^{13}\exp(-3.42\ \text{eV}/k_BT)\ \text{s}^{-1}$ is used and the product is a π-bond. The rate constant of molecular H_2 desorption is taken directly from a temperature programmed desorption experiment[60] with $k=10^{13}\exp(-3.14\ \text{eV}/k_BT)\ \text{s}^{-1}$ and the only mechanistic assumption made about the process is that the two hydrogen atoms must desorb from the same dimer on the surface. In a recent time of flight and recoil spectroscopy (TOF-SARS) experiment,[61] isothermal H_2 desorption is also a first order process with an activation energy of 2.98 ± 0.26 eV and a prefactor of $\approx10^{11}\ \text{s}^{-1}$. Our chosen value of k for H_2 desorption is same as the TPD experimental value.[60] The slower prefactor in TOF-SARS experiment is an average over the full range of experimental conditions where as 10^{13}/s is a suitable prefactor for each independent event.

D. Reverse reactions

In order to satisfy the principle of microscopic reversibility in the TDMC simulations, we must also consider the reverse processes of H_2 depositing a H atom or a H_2 molecule on the surface [Fig. 1(C)]. These processes are too slow to be modeled with MD and the values have not been measured, therefore the rate constants have been estimated from their relative reaction energetics. If we express all of the rate constants in an Arrhenius form and assume a similar prefactor, then it is straightforward to estimate the rate constant of the reverse reaction once the forward rate constant and the relative energetics of the reactants and products is known. If the forward rate constant, k_f, has an activation energy, E_a, and a prefactor, A, then

$$k_f=A\ \exp(-E_a/k_BT). \tag{3}$$

Since the difference in energy between the reactants and products, ΔE, is known, the reverse rate constant can be written as

$$k_r=A\ \exp[-(E_a+\Delta E)/k_BT]. \tag{4}$$

From Eqs. (2) and (3) it is straightforward to determine that

$$k_r=k_fS\ \exp(-\Delta E/k_BT), \tag{5}$$

where, in addition to the energy difference correction, we have also included a steric correction factor, S, to account for any possible steric hindrance in the reverse reaction.

Studies using transition state theory for calculating the rates of H_2 deposition of a H atom on the {111} surface of diamond indicate that in order for the reaction to proceed, H_2 must be almost perfectly collinear with the final C–H bond and aimed right at it.[62] Correspondingly we attempt to account for the area of the carbon atom within the unit cell and the angle at which the deposition takes place on the {001}(2×1) surface. In order for deposition to take place, the H_2 molecule must hit a surface carbon atom. The surface carbon atom occupies approximately 1.81 Å^2 of a 6.37 Å^2 unit cell giving the area correction factor of 1.81/6.37. Assuming the transition state for the reverse reaction is the same as for the forward reaction a polar angle correction factor is applied to take into account that the deposition process is most likely to occur in a collinear fashion. This correction factor of 10°/90° allows the H_2 to impinge at an angle plus or minus ten degrees of collinear. Thus S is approximately 0.03.

Finally the calculated rate constants as described above must be multiplied by the appropriate collision number as defined by Eq. (1). In these cases the mass is that of the H_2 molecule and a H_2 partial pressure of 18 Torr.

There are several approximations here so ultimately the question is whether these will significantly alter the results. The partial pressure of H_2 is typically 10–100 times larger than that for atomic H. The mass factor $(1/\sqrt{2})$ from Eq. (1) and the steric factor (0.03) almost cancel the pressure effect, thus, the dominant term is the exponential of $(\Delta E/k_BT)$. The ΔE values for the three reactions are given in Table III along with the evaluated exponential factors at the temperatures of interest. In the case of deposition of a H atom at an isolated radical ($C5$ in Table I and reverse of H abstraction from a H saturated dimer), the probability of deposition is two orders of magnitude smaller than the competing process of direct H atom adsorption ($A1$). Since both processes have the same end result, the addition of a H atom to a radical site, the exact value for the deposition as a reverse of H abstraction is relatively unimportant. In the other two cases the reverse reac-

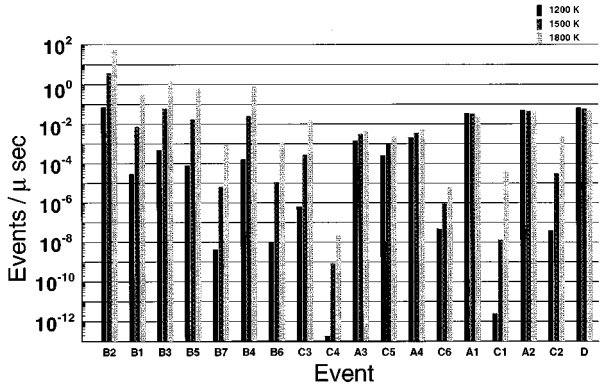

FIG. 4. Histograms of all event probabilities at 1200, 1500, and 1800 K in events/μs/site. The events are labeled as they are given in Fig. 1, with *D* standing for the H collision probability with the diamond surface.

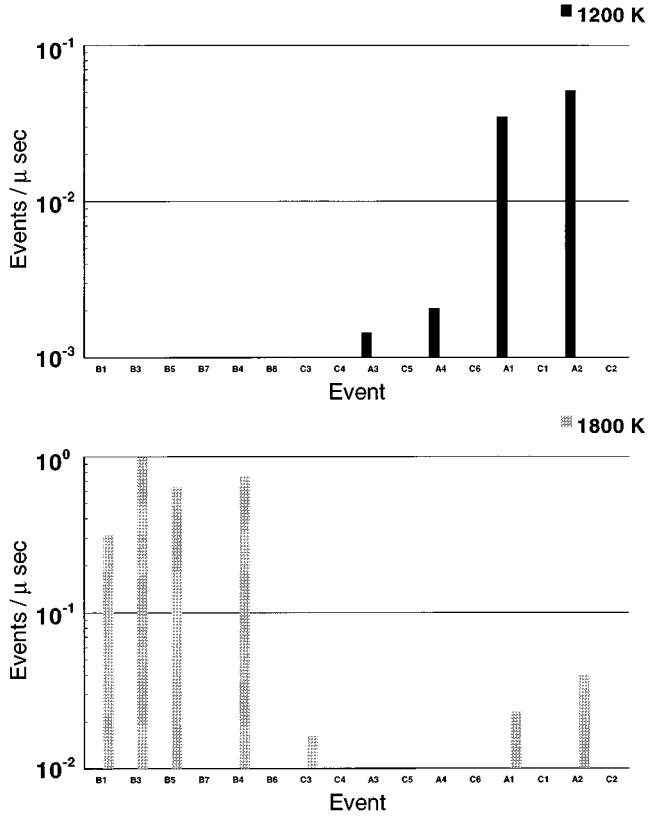

FIG. 5. Histograms of the dominant event probabilities at 1200 and 1800 K. Labeling is the same as for Fig. 4.

tions rates are orders of magnitude less than the corresponding forward reactions and should be negligible.

E. Comparative rates

Before discussing the TDMC calculations it is useful to obtain a perspective of the relative magnitudes of the various processes. Given in Table I are the rates for the various events at 1200, 1500, and 1800 K. The experimental growth conditions are in the lower half of this temperature range. The calculation at the higher temperature (1800 K) is included to account for the possibility that the surface diffusion activation barriers obtained from the empirical potential may be higher than the actual barriers as explained in Sec. II B. The rates are given as number of events per μs per site as this gives a convenient comparative time scale. The rates are displayed graphically in Fig. 4.

In Fig. 5 only the rates of the dominant events at 1200 and 1800 K are shown. At 1200 K the dominant processes are H atom addition to both isolated radicals and π-bonds, events which occur at the rate of approximately 0.04 adsorptions per μs. The H abstraction probabilities are an order of magnitude smaller. The diffusion rates are negligible. One would expect in the TDMC simulations that the total number of radicals would be low and that there would be minimal diffusion of radicals.

At 1800 K the H_2 desorption probability is comparable to the two H adsorption probabilities. This would indicate that the total radical site density should increase. In addition, the diffusion rates are competitive in value and considerable diffusion is expected. Although is it straightforward to estimate the dominant processes from the table of rates, it is almost impossible to predict quantitatively the competitive and cooperative effects.

III. TIME DEPENDENT MONTE CARLO CALCULATIONS

Given an ensemble of microscopic reactions in a system, the essence of the time dependent Monte Carlo calculation is how the system evolves towards the equilibrium configuration. A template or grid of sites is established on which the individual reactions occur. The sites are cycled through, and from a Monte Carlo approach various events are allowed to proceed. Since we are considering a multitude of competing processes for many particles simultaneously, an important consideration is the method by which we extend the Monte Carlo calculation into the time domain. For a single-particle, multiprocess system we use the rates of the microscopic processes to determine the duration of the processes. There is only one clock which keeps track of time for the entire system.[15] The rates of all of the allowed processes for the particle are combined to obtain a total rate and the time step in which the particle moves is then the inverse of the total rate. At each time step, one of all the possible processes is randomly selected and the selected process is allowed to occur with a probability which is the product of the time step and the rate of the individual process.[15] The rates of the individual processes are thus included only through the probabilities in a single time step which is the real time itself. Since the processes are randomly selected both the rare and frequent events are uniformly sampled at each step although the probability of the rare events occurring is very small. The method has been applied successfully to the case of Si adatom diffusion on Si and Ge surfaces.[15,63,64] Recently we have extended this method to a many-particle multiprocess system.[16] The extension is based upon the observation that given the rate of each individual process in a system, the probability of a process occurring within *any* specified time period or time step is simply the product of the time step and

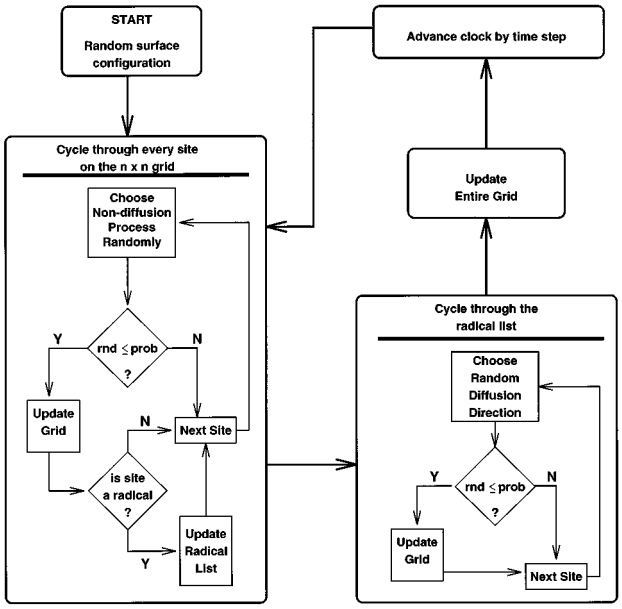

FIG. 6. Flow chart of the TDMC algorithm.

the rate for the process. A single constant time step, δt, for the overall dynamics is chosen such that it is less than the duration of the fastest process considered. The probabilities for all of the considered processes are thus between 0 and 1. All of the particles are allowed to move in each step with the process for each particle randomly selected. A particle moves, however, only if the probability of the move is less than a uniformly sampled random number between 0 and 1. The constant time step is chosen such that the acceptance probability of the fastest process is about 0.5, a value typical of most MC simulations. With this procedure, values of $\delta t = 10^{-5}$ s (1200 K), 10^{-7} s (1500 K), and 10^{-8} s (1800 K) are chosen. The time step $\delta t = 10^{-5}$ s at 1200 K, however, is larger than the lifetime of a single radical. A $\delta t = 10^{-7}$ s which is smaller than the lifetime of a radical is used in the simulation at 1200 K. The results for radical diffusion (Fig. 7) were generated with time steps chosen from our earlier approach[15] because a single radical diffusion in a many-particle multiprocess system can be treated like a tracer diffusion in the system.

A comparison of the above method with other recent TDMC approaches for many-particle, multiprocess systems[18,19,25–29] is now in order. Given the rates and probabilities for each process in the system, in one approach [18,19] the time step is the inverse of the net total reaction rate. At each step a particle with a process is selected with a probability based on the individual rate. The process is allowed to occur while other particles remain stationary. In other approaches[25,26] each particle is assigned an independent time clock. The clock for each particle advances as the reciprocal of the rate of the process that occurs. A master clock keeps track of the overall time, particles move consecutively such that a particle moves only when sufficient time has passed.[25,26] The relationship between the time kept on individual atomic clocks and on the master clock with real experimental time remains unclear and is considered as an average over all of the particles. The approach in Ref. 27 picks particles randomly, from a list of given transition type, but the relationship of the individual time steps with an overall real time step is also considered as an average over all the particles in the system. In our approach there is only one time which is the real time itself. At each step all particles are allowed to move, albeit probablistically, and events for the particle are randomly sampled. The inconsistencies in the independent and master clock method[25–27] have been identified and addressed in recent publications.[28,29] In the refined method[28] for Poisson processes, the transition probabilities are constructed from the normalization of individual rates and the time step is the inverse of the average rate weighted by a Poisson probability distribution. The particles are randomly selected and the time step is incremented only for successful moves. When rare events occur, they are necessarily accompanied by long time increments. Our method allows for rare events happening at short time duration although with small probability. This is in principle closer to the philosophy of static MC methods where atomic configurations of higher energies are also accepted albeit with small probability. Cao in Ref. 29 points out that in the case of independent and master clock methods, a faster convergence is achieved if the real time step is an average over all the processes in the system and not over all the particles in the system as considered in Refs. 25–27. For a single particle many process system, in such a case, Cao's method is the same as our approach.[16] The rare events in our approach though are uniformly sampled as real time progresses.

We are interested in the dynamics of hydrogen on a diamond $\{001\}(2\times1)$ surface with the goal of determining the radical site density and distribution. The grid chosen is 100×100 points with periodic boundary conditions in which each grid point is a $\{001\}(2\times1)$ surface C atom either with or without a bonded H atom. The algorithm followed for this calculation is given schematically in Fig. 6. The TDMC calculation proceeds by keeping track of all the grid points as well as a history of each radical. In a single time step all grid points are checked for the possible adsorption, desorption, or abstraction events which affect the radical density. Since the radicals are constantly created or destroyed at each grid point, the radical list at each step is sufficiently uncorrelated with the list of the previous step. The complete list of radicals at each step is thus cycled through and checked for diffusion. This approach assumes a separation of the diffusive events from all of the other events considered. This assumption is deemed reasonable as the overall radical concentration before and after the diffusive events remains the same. The model allows for the tabulation of the overall radical and π-bond concentrations as well as the diffusion constants and lifetimes for each species.

A. Diffusion of a single isolated radical vs temperature and CH_3 coverage

The diffusion of a single species, i.e., a radical, on the $\{001\}(2\times1)$:H surface is the simplest of the TDMC simulations performed and is similar to those performed for Si and Ge adatoms on Si surfaces.[15,63,64] Shown in Fig. 7 is the

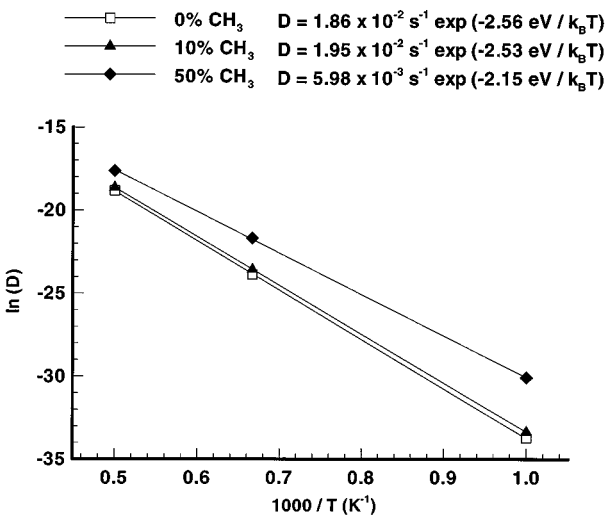

FIG. 7. Arrhenius plot of diffusion constants for an isolated radical diffusing on a diamond {001}(2×1):H surface with three different CH_3 coverages; Θ=0.00, Θ=0.10, Θ=0.50.

temperature dependence of the radical site diffusion. It displays Arrhenius behavior with an activation energy of 2.56 eV, a value indicative of the diffusion barrier for a H atom along the dimer row. The diffusion is anisotropic but at this stage we do not feel that the reliability of the relative activation energies is such that we wish to attach significance to the directionality. The TDMC method is capable, though, of determining the specific amounts of anisotropy.[15,63]

The effect of 10% and 50% CH_3 coverage on the radical diffusion is also shown in Fig. 7. The united CH_3 species serves as a trap for radical diffusion at low CH_3 coverages. That is, the fastest diffusion reaction is for the radical and the CH_3 species to exchange places but then the fastest motion for the next move is for the same radical and CH_3 species to re-exchange back to the original configuration. Consequently there is no net diffusive motion. This interpretation is consistent with the data in Fig. 7 which have the diffusion rate for the 10% CH_3 coverage to be nearly identical with the fully hydrogen terminated surface. By increasing the CH_3 coverage to 50% many slower diffusing H are replaced by faster diffusing CH_3. Alternative easy diffusion paths are presented to the radical and the radical diffusion rate increases.

B. Equilibrium configuration and radical dynamics

The full TDMC simulation consists of all the H atom and H_2 molecule steps for addition and subtraction of H atoms to the surface as well as migration on it. The strength of the TDMC approach is that all these processes can be included regardless of the time scale. The inherent danger of any TDMC approach is that one might not include ''all'' the important events. In fact, our initial study assumed that there were only isolated radicals on the surface. It was after examining the final configuration that we realized the importance of π-bonds and accordingly have calculated more energetics and included more events in the TDMC calculation. The presence of the π-bonds offer the possibility of faster CH_3 adsorption onto the surface and incorporation into the diamond lattice.[16]

The results from the full TDMC simulation of H motion on the {001}(2×1):H surface are given in Table IV. The concept of radical diffusion now becomes radical lifetime. The isolated radical coverage is given as a percentage of all available C atom sites. The π-bond coverage is given as a percentage of surface dimers. For example, at 1800 K with a H partial pressure of 0.10 Torr, 22% of 100 000 C atom sites are radicals or there are 22 000 isolated radicals. In addition, 12% of the 50 000 possible surface dimers are π-bonds, thus there are 6000 π-bonds. Consequently there are ~66 000 H atoms bound on the surface.

The values of the lifetimes and coverages at a H partial pressure of 0.10 Torr are logical based on the probability of the events as given in Table III. The radical lifetime is almost independent of temperature and has a value of 30 μs. This corresponds to a migration area of approximately 120 Å^2 at 1800 K or approximately 50 hops. The radical is annihilated by adsorption of a H atom from the gas phase. The lifetime of the π-bond is 10 μs. The π-bond does not diffuse. It is created by either two radicals diffusing together, H_2 desorption, or the removal of a H atom, from a dimer with only one H atom, by way of abstraction. It is annihilated by adsorption of a H atom from the gas phase and by the diffusion of a H atom onto the π-bond. As expected the radical coverage increases with temperature as H_2 desorption becomes relatively more important at higher temperatures (Fig. 5, Table III). Similarly the π-bond coverage increases with temperature.

The validity of these conclusions must be ascertained against the assumptions/limitations of the empirical potential. To this end, the TDMC calculations have been repeated for H atom partial pressures an order of magnitude larger (1

TABLE IV. Radical and π-bond lifetimes and coverages as a function of temperature and H partial pressure.

H partial pressure (Torr)	0.01			0.10			1.00		
Temperature (K)	1200	1500	1800	1200	1500	1800	1200	1500	1800
Radical lifetime (μs)	261	260	213	28	30	31	3	3	4
π-bond lifetime (μs)	100	108	109	10	11	12	1	1	1
Radical coverage (%)	3.8	11	33	3.8	9	22	3.8	8.3	16
π-bond coverage (%)	0.2	3	25	0.2	1	12	0.2	0.7	3

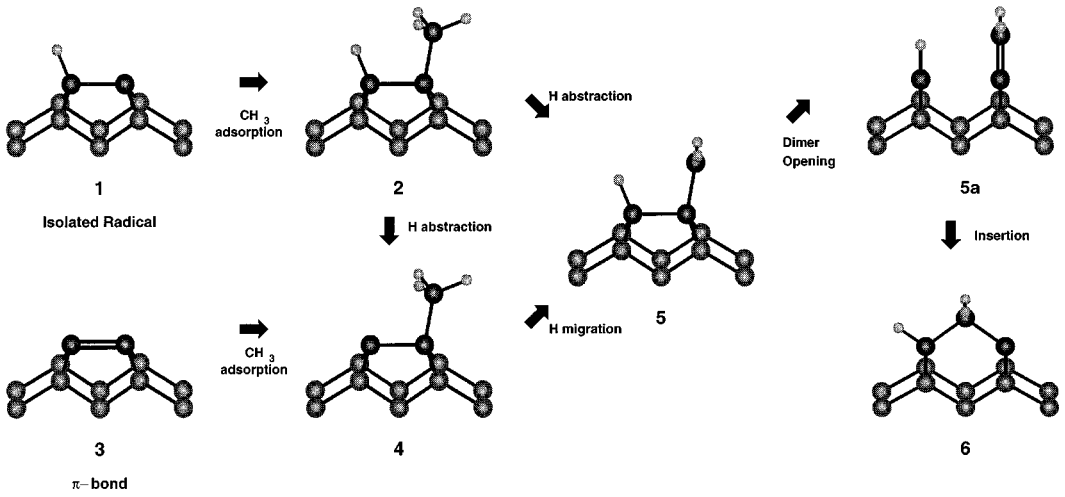

FIG. 8. The pathways for CH_2 insertion into a dimer epitaxial site.

Torr) and smaller (0.01 Torr) than the initial calculation. As given in Table IV the pressure variation only changes the radical and π-bond coverages by about a factor of 1–2 in each direction. The H partial pressure does affect the lifetimes of both the radical and π-bond by an order of magnitude in each direction. Not surprisingly the more H that is present in the plasma, the shorter the lifetime of the radicals. The uncertainty in the diffusion barriers, as mentioned above, has been compensated for in two ways. First, the TDMC simulations have been performed at elevated temperatures compared to the typical diamond growth temperatures. In all cases this leads to increases in the percentage of π-bonds on the surface. Second, the calculations were repeated for diffusion barriers 0.8–1 eV lower in the direction across the trough. This adjustment does not affect the total number of radicals but does predict that the percentage of π-bonds increases at the expense of isolated radicals. In none of the calculations did the π-bonds disappear.

IV. COMMENTS

A many-particle multiprocess TDMC method has been developed for two-dimensional reactive systems. This approach allows one to use molecular dynamics simulations to search for reaction mechanisms[17] and also to calculate probabilities of short time events such as adsorption and abstraction. Transition state theory is used to calculate rates of slow events such as diffusion. Finally the time dependent Monte Carlo simulations take the microscopic information into the realm of macroscopic observables.

This prescription has been applied to the reactions of hydrogen atoms and molecules on the diamond $\{001\}(2\times1)$ surface. Radical site densities and lifetimes are readily calculable. Moreover, the simulations predict the presence of π-bonds on the surface. This second form of reaction center, in addition to the isolated radical, presents alternative pathways for carbon incorporation into the diamond lattice.[16]

It has been proposed that a key step for diamond film growth is the insertion of a CH_2 species initially adsorbed on one of the surface dimer C atoms into the surface dimer (configurations 5 and 6 of Fig. 8), thus adding one C atom in an epitaxial position.[17] If only isolated radicals are present as reaction centers, as previously postulated,[1–13] the formation of the adsorbed CH_2 unit (configuration 5) can occur via two pathways as shown in Fig. 8. In path 1-2-5 and 1-2-4-5, adsorption of CH_3 at the isolated radical is followed by H abstraction from the adsorbed CH_3. On the other hand, if strained π-bonds are also present on the surface, the CH_3 can add to a π-bond (path 3-4-5) and a H atom can migrate to the resultant adjacent radical by either an intra- or intermolecular mechanism.[33] The difference in importance among the paths 1-2-5, 1-2-4-5, and 3-4-5 depends on the concentrations of the isolated radical (configuration 1) vs the π-bond (configuration 3), the rates of CH_3 addition to the two reaction centers, and the relative rate of H abstraction (path 2-5 or 2-4) vs H migration (path 4-5). The adsorption of CH_3 at the π-bond (i.e., path 3 to 4) is about an order of magnitude larger than at the isolated radical (path 1 to 2), whereas the π-bond concentration is about an order of magnitude less than the isolated radical concentration. Thus the key factor which influences the relative rates among the three reaction paths in Fig. 1 is the H abstraction probability in path 2 to 5 or 2 to 4 vs the H migration probability in path 4 to 5. Abstraction of a H atom at a partial pressure of 0.1 Torr and in the temperature range of 1200–1800 K occurs about once every millisecond per site. A simple transition state theory estimate of H migration suggests that it should occur once every nanosecond per site. Since the reaction from 5 to 6 occurs once per picosecond per site we estimate that the formation of CH_2 adspecies through the π-bond site in scheme 3 is 4 to 6 orders of magnitude faster than through the isolated radical in scheme 1.

The extension of this approach into the realm of three-dimensional growth is the real challenge. Work currently in progress includes events associated with the small hydrocarbon species necessary for diamond growth. Additionally the system will include not only the two-dimensional surface,

but also the three-dimensional diamond lattice. This approach provides the framework necessary to simulate CVD growth processes.

ACKNOWLEDGMENTS

We gratefully acknowledge financial support from the Office of Naval Research. We thank Professor Ken S. Feldman for insightful conversations on organic chemistry and diamond film growth processes. The computational support for this work was provided by the IBM-SUR program at the Penn State University.

[1] R. Haubner and B. Lux, Diamond Relat. Materials **2**, 1277 (1993).
[2] C.-P. Klages, Appl. Phys. A **56**, 513 (1993).
[3] J. C. Angus, A. Argoitia, R. Gat, Z. Li, M. Sunkara, L. Wang, and Y. Wang, Philos. Trans. R. Soc. London, Ser. A **342**, 195 (1993).
[4] See, for example, J. E. Butler and R. L. Woodin, Philos. Trans. R. Soc. London, Ser. A **342**, 209 (1993), and references therein.
[5] S. J. Harris and D. G. Goodwin, J. Phys. Chem. **97**, 23 (1993).
[6] M. Tsuda, M. Nakajima, and S. Oikawa, J. Am. Chem. Soc. **108**, 5780 (1986).
[7] M. Tsuda, M. Nakajima, and S. Oikawa, Jpn. J. Appl. Phys. **26**, L527 (1987).
[8] M. Frenklach and K. E. Spear, J. Mater. Res. **3**, 133 (1988).
[9] M. Frenklach and H. Wang, Phys. Rev. B **43**, 1520 (1991).
[10] P. Deak, P. Giber, and H. Oechsner, Surf. Sci. **250**, 287 (1991).
[11] B. H. Besler, W. L. Hase, and K. C. Hass, J. Phys. Chem. **96**, 9369 (1992).
[12] J. E. Butler and R. L. Woodin, Phys. Trans. R. Soc. London, Ser. A **342**, 209 (1993).
[13] M. E. Coltrin and D. S. Dandy, J. Appl. Phys. **74**, 5803 (1993).
[14] D. W. Brenner, K. J. Tupper, J. A. Harrison, and B. I. Dunlap (preprint, 1993).
[15] D. Srivastava and B. J. Garrison, J. Chem. Phys. **95**, 6885 (1991).
[16] E. J. Dawnkaski, D. Srivastava, and B. J. Garrison, Chem. Phys. Lett. **232**, 524 (1995).
[17] B. J. Garrison, E. J. Dawnkaski, D. Srivastava, and D. W. Brenner, Science **255**, 835 (1992).
[18] A. F. Voter, Phys. Rev. B **34**, 6819 (1986).
[19] D. T. Gillespie, J. Phys. Chem. **81**, 2340 (1977).
[20] Z. Zhang and H. Metiu, Surf. Sci. Lett. **292**, L781 (1993).
[21] P. W. Rooney and F. Hellman, Phys. Rev. B **48**, 3079 (1993).
[22] J. Xing and H. L. Scott, Phys. Rev. B **48**, 4806 (1993).
[23] J. Cortes, E. Valencia, and P. Araya, J. Chem. Phys. **100**, 7672 (1994).
[24] S. Pal and D. P. Landau, Phys. Rev. B **49**, 10 597 (1994).
[25] H. C. Kang and W. H. Weinberg, J. Chem. Phys. **90**, 2824 (1989).
[26] L. A. Ray and R. C. Baetzold, J. Chem. Phys. **93**, 2871 (1990).
[27] A. M. Bowler and E. S. Hood, J. Chem. Phys. **94**, 5162 (1991).
[28] K. A. Fichthorn and W. H. Weinberg, J. Chem. Phys. **95**, 1090 (1991).
[29] P. L. Cao, Phys. Rev. Lett. **73**, 2595 (1994).
[30] D. W. Brenner, Phys. Rev. B **42**, 9458 (1990).
[31] See, for example, C. Kress, M. Fiedler, W. G. Schmidt, and F. Bechsted, Phys. Rev. B **50**, 17 697 (1994), and references therein.
[32] B. Weiner, S. Skokov, and M. Frenklach, J. Chem. Phys. **102**, 5486 (1995).
[33] S. Skokov, B. Weiner, and M. Frenklach, J. Phys. Chem. **98**, 8 (1994).
[34] E. J. Dawnkaski, D. Srivastava, and B. J. Garrison (in preparation).
[35] D. W. Brenner, J. A. Harrison, C. T. White, and R. J. Colton, Thin Solid Films **206**, 220 (1991).
[36] E. R. Williams, G. C. Jones, Jr., L. Fang, R. N. Zare, B. J. Garrison, and D. W. Brenner, J. Am. Chem. Soc. **114**, 3207 (1992).
[37] R. S. Taylor and B. J. Garrison, J. Am. Chem. Soc. **116**, 4465 (1994).
[38] R. S. Taylor, C. L. Brummel, N. Winograd, B. J. Garrison, and J. C. Vickerman, Chem. Phys. Lett. (in press).
[39] R. S. Taylor and B. J. Garrison, J. Langmuir (to be published).
[40] R. S. Taylor and B. J. Garrison, Chem. Phys. Lett. **230**, 495 (1994).
[41] R. S. Taylor and B. J. Garrison, Int. J. Mass Spectrom. Ion Proc. (to be published).
[42] J. A. Harrison, D. W. Brenner, C. T. White, and R. J. Colton, Thin Solid Films **206**, 213 (1991).
[43] J. A. Harrison, C. T. White, R. J. Colton, and D. W. Brenner, Surf. Sci. **271**, 57 (1992); J. A. Harrison, R. J. Colton, C. T. White, and D. W. Brenner, Mater. Res. Soc. Symp. Proc. **239**, 573 (1992).
[44] D. W. Brenner and J. A. Harrison, Am. Ceram. Soc. Bull. **71**, 1821 (1992).
[45] J. Peploski, D. L. Thompson, and L. M. Raff, J. Phys. Chem. **96**, 8538 (1992).
[46] X. Chang, D. L. Thompson, and L. M. Raff, J. Phys. Chem. **97**, 10 112 (1993).
[47] X.-Y. Chang, D. L. Thompson, and L. M. Raff, J. Chem. Phys. **100**, 1765 (1994).
[48] M. D. Perry and L. M. Raff, J. Phys. Chem. **98**, 4375 (1994).
[49] M. D. Perry and L. M. Raff, J. Phys. Chem. **98**, 8128 (1994).
[50] H. J. C. Berendsen, J. P. M. Postawa, W. F. van Gunsteren, A. Dinola, and J. R. Haak, J. Chem. Phys. **81**, 3684 (1984).
[51] D. W. Brenner, D. H. Robertson, R. Carty, D. Srivastava, and B. J. Garrison, Mater. Res. Soc. Proc. **278**, 255 (1992).
[52] T. A. Schoolcraft and B. J. Garrison, J. Vac. Sci. Technol. A **8**, 3496 (1990).
[53] X. Y. Chang, M. Perry, J. Peploski, D. L. Thompson, and L. M. Raff, J. Chem. Phys. **99**, 4748 (1993).
[54] P. W. Atkins, *Physical Chemistry*, 3rd ed. (Freeman, New York, 1986), p. 764.
[55] W. L. Hsu, Appl. Phys. Lett. **59**, 1427 (1991).
[56] C. Choi and R. Elber, J. Chem. Phys. **94**, 751 (1991).
[57] J. D. Winkler, V. Sridar, L. Rubo, J. P. Hey, and N. Haddad, J. Am. Chem. Soc. **54**, 3004 (1989).
[58] There are two possible significant differences between small molecule chemistry and the diamond surface. First, the temperatures for diamond growth are much higher. The rate for the 1,2 radical shift at 300 K from the activation energies in the table is 10^{-21} per s. Presumably this rate is so slow that other reactions occur first. Second, the number of available competing reactions may be much more limited in the diamond film.
[59] K. S. Feldman (private communication).
[60] R. E. Thomas, R. A. Rudder, and R. J. Markunas, J. Vac. Sci. Technol. A **10**, 2451 (1992).
[61] D. D. Koleske, S. M. Gates, B. D. Thomas, J. N. Russell, Jr., and J. E. Butler, J. Chem. Phys. **102**, 992 (1995).
[62] R. L. Carty, Masters thesis, Penn State University, 1993.
[63] D. Srivastava and B. J. Garrison, Phys. Rev. B **46**, 1472 (1992).
[64] D. Srivastava and B. J. Garrison, Phys. Rev. B **47**, 4464 (1993).